Life Sciences 226 (2019) 57–67

Contents lists available at ScienceDirect

Life Sciences

journal homepage: www.elsevier.com/locate/lifescie

Temporal analysis of distribution pattern of islet cells and antioxidant enzymes for diabetes onset in postnatal critical development window in rats

Franciane Quintanilha Gallego[a], Carolina Abreu Miranda[a], Yuri Karen Sinzato[a], Isabela Lovizutto Iessi[a], Bruna Dallaqua[b], Rogelio Hernandez Pando[c], Noeme Sousa Rocha[d], Gustavo Tadeu Volpato[e], Débora Cristina Damasceno[a,*]

[a] Laboratory of Experimental Research of Gynecology and Obstetrics, Postgraduate Course of Gynecology, Obstetrics and Mastology, Botucatu Medical School, São Paulo State University (UNESP), Botucatu, São Paulo, Brazil
[b] DeVry Ruy Barbosa School (DeVry Brazil Group), Salvador, Bahia State, Brazil
[c] Department of Pathology, National Institute of Medical Sciences and Nutrition "Salvador Zubirán", Mexico City, Mexico
[d] Department of Pathology, School of Veterinary Medicine and Animal Science (FMVZ), São Paulo State University (UNESP), Botucatu, São Paulo, Brazil
[e] Laboratory of System Physiology and Reproductive Toxicology, Institute of Biological and Health Sciences, Federal University of Mato Grosso (UFMT), Barra do Garças, Mato Grosso State, Brazil

ARTICLE INFO

Keywords:
Insulin
Somatostatin
Glucagon
Oxidative stress
Rats

ABSTRACT

Aim: At performing a temporal analysis of the distribution pattern of islet endocrine cells and antioxidant enzymes in diabetic rats during the post-natal critical development window.
Main methods: The newborns received streptozotocin (STZ) at birth for diabetes induction, and control females received the vehicle. The animals were euthanized at different lifetimes: D5, D10, D15, and D30. Morphological analysis of pancreas and biochemical assays was performed.
Key findings: The STZ-induced rats presented irregular shape of islet on D5 and there was an attempt to restore of this shape in other life moment studied. There was an increase progressive in islet area, however they maintained smaller than those of control rats, with lower labeling intensity for insulin, higher for glucagon and somatostatin, lower for SOD-1 was lower in the islets of the STZ-induced animals at all times studied and for GSH-Px in D10 and D30.
Significance: Although STZ-induced diabetic rats presented compensatory mechanisms to restore the mass of endocrine cells, this was not sufficient since these rats developed the diabetic state. This was confirmed by the oral glucose tolerance test from D30. In addition, the delta (δ)-cells presented ectopic location in islets, indicating a possible relationship for beta (β)-cell mass restoration. There was a response of the pancreas to reduce the hyperglycemia in the first month of life. Furthermore, the cells from the endocrine pancreas of diabetic animals show a decline of antioxidant enzymatic, contributing to the increased susceptibility of cells to hyperglycemia-induced ROS in this postnatal critical development window.

1. Introduction

Pancreatic islets are specialized endocrine micro-organs composed of cells alpha α (glucagon), beta β (insulin), delta δ (somatostatin), PP (pancreatic polypeptide), and epsilon Ɛ (ghrelin) [1]. These cells communicate via GAP junction or a paracrine pathway [2]. The cytoarchitecture of mouse and human pancreatic islets is similar, in both showing a mantle-core pattern in which β-cells are surrounded by non-β-cells [3].

In mammalian species, most α- and δ-pancreatic cells are aligned along blood vessels. This close contact with capillary blood vessels enable these cells to sense changes in glucose which are communicated from non-β to β-cells through blood to regulate insulin secretion [4–8]. Thus, insulin and glucagon together regulate glucose homeostasis as glucagon increases blood glucose levels, whereas insulin decreases it when necessary [1]. Somatostatin inhibits both glucagon and insulin release and, therefore, plays an indirect role in glucose regulation [9].

There is evidence that hyperglycemia increases the production of reactive oxygen species (ROS) by increasing the flux of electron donors into the mitochondrial electron-transport chain [10]. ROS plays an important role in the pathogenesis of β-cell loss in *Diabetes mellitus* (DM). When glucose concentration rises, β-cells increase their oxidative

* Corresponding author at: Departamento de Ginecologia e Obstetrícia – FMB, UNESP, Distrito de Rubião Júnior s/n, CEP. 18618-687 Botucatu, São Paulo, Brazil.
E-mail address: damascenofmb@gmail.com (D.C. Damasceno).

https://doi.org/10.1016/j.lfs.2019.03.061
Received 14 January 2019; Received in revised form 12 March 2019; Accepted 25 March 2019
Available online 28 March 2019

glucose catabolism, which causes insulin synthesis and secretion to permit glucose to be used by the peripheral tissues [11]. Insulin-producing cells have a particularly low antioxidative defense capacity with a very low expression of the antioxidant enzymes superoxide dismutase (SOD) and glutathione peroxidase (GSH-Px) [12,13]. Thus, β-cells are the most susceptible to oxidative stress, which affects insulin expression and secretion as well as increases apoptosis aggravating the hyperglycemic state [14].

Diabetes has been induced by beta-cytotoxic drug streptozotocin (STZ) in the laboratory animal models. STZ presents glucose component, is stored in beta (β) cells through glucose transporter type 2 (GLUT 2) in the plasma membrane [11,15]. GLUT-2 is expressed in the majority of pancreatic β-cells and is not expressed in non-β-cells (α and δ) of the rat islets [16]. Thus, STZ affects insulin synthesis and secretion through three mechanisms inducing β-cell death: DNA methylation by carbonium ion ($CH3^+$) formation, which triggers poly (ADP-ribose) synthetase; nitric oxide production; and free radical generation in the plasma membrane [15,17].

For mild diabetes induction, the rats receive STZ during neonatal period. The diabetic animals present glycemic levels at adulthood similar to Type 2 *Diabetes mellitus* and/or human Gestational *Diabetes mellitus* [18]. The neonatal period is considered as a critical development window for the pancreas in mammals. In lactating rats, there is a higher consumption of carbohydrates and lipids, which stimulates the endocrine pancreas and increases the rate of β-cell proliferation [19,20], reduces glucose sensitivity and insulin secretion [20]. For this reason, the lactation period is considered a period of pancreatic remodeling. Several studies using STZ in neonatal period as diabetes model have been conducted to understand how β-cell regeneration occurs after injury [21–25]. STZ-injected rat in neonatal period showed that the islets undergo a rapid regeneration with generation of new islets and restructuring of preexisting islets. In addition, glucagon-positive cell hyperplasia has been observed, which probably reflects the homeostatic stimulus to restore cell mass that becomes age-limiting [26].

The structural and functional changes on the rat pancreatic islets after birth clearly indicate that this period is a critical development window in rats. In addition, some of these changes can cause diseases, such as diabetes in adulthood. However, there is no evidence of the involvement of antioxidant defenses in these alterations in pancreatic islets after β-cell injury. Thus, in order to improve our understanding of islet structural and functional changes, this study aimed at performing a temporal analysis of the distribution pattern of islet endocrine cells and antioxidant enzymes in diabetic rats during the post-natal critical development window.

2. Materials and method

2.1. Animals

Wistar rats were maintained under controlled conditions of temperature (22 ± 2 °C), humidity (50 ± 10%) and light/dark cycle (12 h) in the Laboratory of Experimental Research in Gynecology and Obstetrics. Filtered water and feed were offered ad libitum. These rats were mated with normoglycemic males (ratio of two females and one male rat) to obtain newborns (NB) for the distribution of non-diabetic (control) and STZ-injected groups (induction of diabetes). The Ethics Committee on Animal Use (CEUA) of Botucatu Medical School/Unesp approved all the experimental procedures applied in this study (Number of Protocol 1219/2017).

2.2. Experimental design

Fig. 1 shows a schematic representation of the experimental design.

2.2.1. Streptozotocin administration

Wistar rats bred in our animal facility were fed ad libitum with commercial rat chow (Purina®, Brazil). Pups were injected with streptozotocin (100 mg/kg, sc., Sigma–Aldrich, St. Louis, MO, USA) diluted in citrate buffer (0.10 M, pH 4.5, Sigma–Aldrich, USA) on day of birth [27] to induce beta cell necrosis, reproducing glycemic levels similar to Type 2 *Diabetes mellitus* or Gestational diabetes. Control animals were injected with citrate buffer alone. In a different way to Gallego et al. [27], in this study as an inclusion criterion, the glycemia of each newborn was determined on day 5 of life (D5) by lancing the tail vein of the animal to obtain a drop of blood. This criterion was used because the animals were killed before adulthood (90 days). The blood sample was read in a conventional glucometer. STZ rats were considered as diabetic when presented a glycemia equal to or > 400 mg/dL on D5, and female offspring that presented no glycemia equal to or lower than 400 mg/dL were discarded. For the control group, female offspring with glycemia < 120 mg/dL on D5 were included [28]. The animals were pseudorandomly assigned (maximum of 5 newborns/mother) to compose different pool per group for the experiment on D5, D10 and D15, and 2 pups/mother on D30.

2.2.2. Experimental groups

The experimental groups were: Control - female newborns rats that received the vehicle citrate buffer in the first day of life (D1), and STZ - female newborns injected with STZ in D1 to induce diabetic status. Animals from both groups were euthanized at days 5 (confirmation of STZ action), 10, 15 (breastfeeding phase), and 30 (post-weaning period). The days 10 and 15 corresponds to the pancreatic regeneration period, while day 30 represents the period immediately after cell regeneration and possible changes related to the weaning period.

2.2.3. Oral glucose tolerance test (OGTT)

At 28 days of life, the D30 groups were submitted to an oral glucose tolerance test (OGTT). Briefly, after six hours of fasting, a drop of blood was collected by venipuncture from the tail for glycemic determination (time 0). Then, rats received glucose solution by intragastric route (2.0 g/kg body weight), and after 30, 60 and 120 min the blood glucose levels were measured and used to estimate the total area under the curve by the mathematic trapezoidal method [29].

2.2.4. Blood and pancreas sample collection

At the studied moments (D5, D10, 15 and 30), the animals were anesthetized with sodium thiopental (Thiopentax®, Cristália, Brazil) and euthanized by decapitation, the blood samples were collected and used to determine insulin, glucagon, and fructosamine in serum. Then, the animals were submitted to laparotomy for the collection of the pancreas for immunolabeling of insulin, glucagon, somatostatin, SOD-1 and GSH-Px.

2.3. Serum insulin, glucagon and fructosamine measurements

The whole blood samples were centrifuged at 1575 × *g* for 10 min at 4 °C, and the obtained serum was stored in a freezer at −80 °C. The insulin (Crystal Chemical® - Code: 90060, USA) and glucagon (Sigma Aldrich® - Code: RAB0202, USA) measurements were determined according to manufacturer instructions of the specific commercial kits. The serum fructosamine concentrations (a biomarker of glycated serum protein) were measured by the Clinical Laboratory of School of Veterinary Medicine and Animal Science (FMVZ), Unesp.

2.4. Morphological analysis of the pancreas

After its dissection, the pancreas was weighed and fixed in 10% formaldehyde for 24 h, dehydrated in progressive alcohol concentrations and embedded in paraffin. Sections of 5 μm width were obtained using a rotary microtome and stained with hematoxylin and eosin for

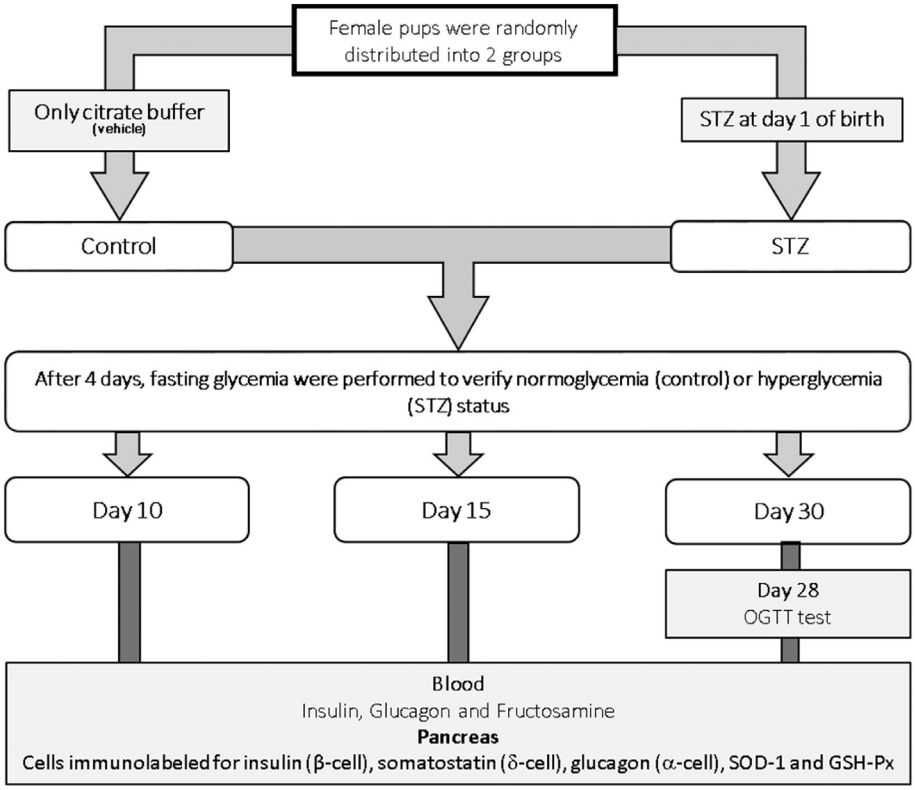

Fig. 1. Experimental design.

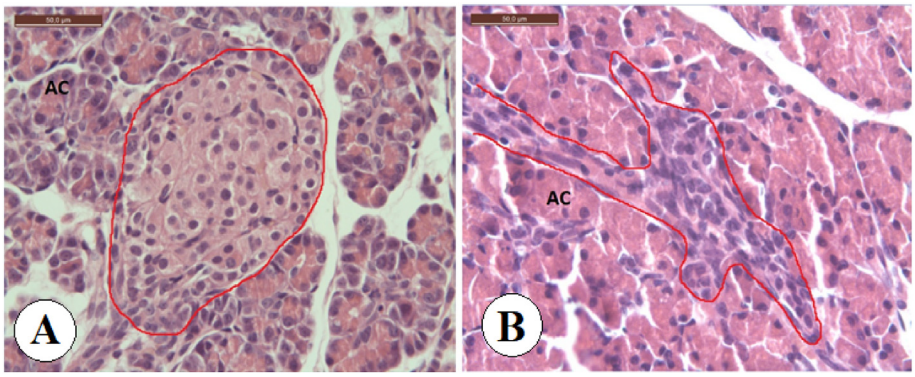

Fig. 2. Pancreatic islets of the control and STZ animals on day 5 (D5) of life (Hematoxilin/Eosin). A- Pancreatic islet in control group (40× magnification). B- Pancreatic islet in STZ group (40× magnification).

conventional histological analysis and measurement of pancreatic islets area. The pancreatic islets were identified and the images were captured using the computerized image system (Software KS-300, version 3.0, Zeiss®), integrated with the digital camera image (CCD-IRIS/RGB, Sony®, China) microscope (DMR, Leica®, Brazil). The images were analyzed through ImageJ® software, and the area was presented in pixels^2. The same material was used for immunohistochemistrical analysis. Each section of 5 μm width was incubated with polyclonal specific antibody against insulin, glucagon, and somatostatin for evaluation of pancreatic islet hormones, and anti-superoxide dismutase 1, and anti-glutathione peroxidase for antioxidant enzymatic analysis. Antigen retrieval was performed in the Elite Bistro® pressure cooker with citrate solution (pH 6.0) for 30 min for anti-insulin and anti-glucagon antibodies and for anti-superoxide dismutase 1, anti-glutathione peroxidase during 20 min. For anti-somatostatin antibody, antigen retrieval was not performed. Endogenous peroxidase (peroxidase inhibitor containing hydrogen peroxide and 15 mM sodium azide - Dako®) blockade was performed for 40 min at room temperature for all antibodies. For the blockade of non-specific proteins, Protein Block (0.25% casein in PBS, containing carrier protein and 15 mM sodium azide - Dako®) was used for 30 min in an oven at 27 °C. Blockade with 8% skim milk (Molico®, Brazil) was used for anti-superoxide dismutase 1 and anti-glutathione peroxidase antibodies for one hour at room temperature. Dilutions for the primary antibodies were: 1: 10,000 anti-insulin (Abcam®, USA, Code: ab8304 incubation for one hour in an oven at 27 °C); 1: 500 anti-glucagon (Abcam®, USA, Code: ab8055 - incubation for two hours in an oven at 27 °C); 1: 2000 anti-somatostatin (Dako®, USA, Code: a0566 - overnight incubation in a refrigerator at 4 °C); 1:200 anti-superoxide dismutase 1 (Abcam®, USA, ab16831–24 h at 4 °C); 1:400 anti-glutathione peroxidase (Abcam®, USA, ab22604-, 24 h at 4 °C). After incubation of the primary antibody, the secondary antibody (Histofine) was added for 30 min in an oven at 27 °C. For the development of peroxidase, the chromogen DAB (3,3-diaminobenzidine) was used for 3 min at room temperature. Then, the slides were

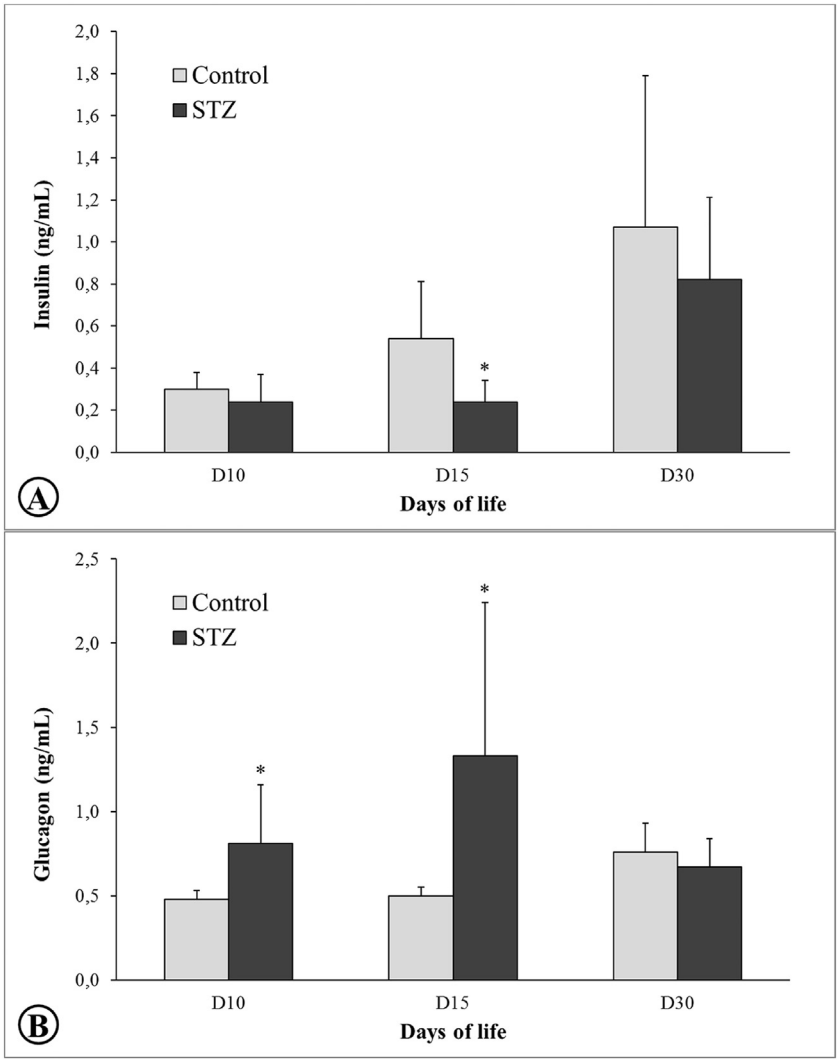

Fig. 3. A - Insulin (mg/dL). B – Glucagon (ng/mL) concentrations in serum of the control and STZ animals at different moments of life (days 10, 15 and 30 of life) (n = 5 animals/group).
Data expressed as the mean ± standard deviation (*Gamma Distribution*).
* p < *0.05 - compared to the Control group*.

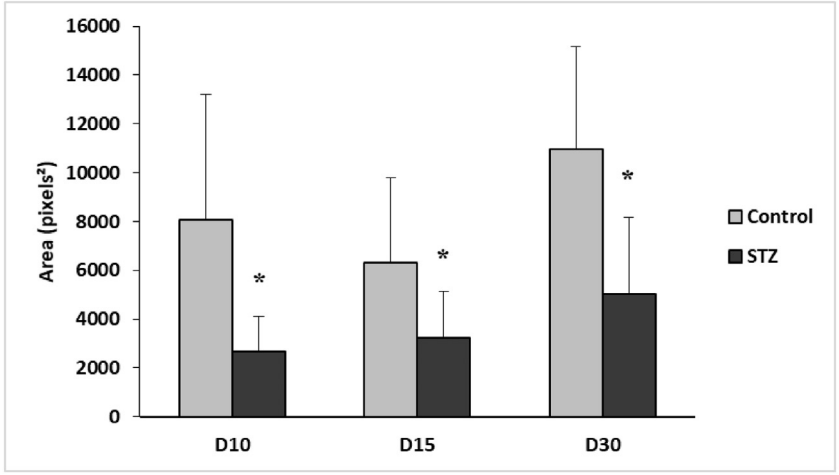

Fig. 4. Pancreatic islet area (pixels^2) in the control and STZ animals.in different moments of life (days 10, 15 and 30 of life).
Data expressed as the mean ± standard deviation (*Poisson Distribution*).
* p < *0.05 - compared to the Control group*.

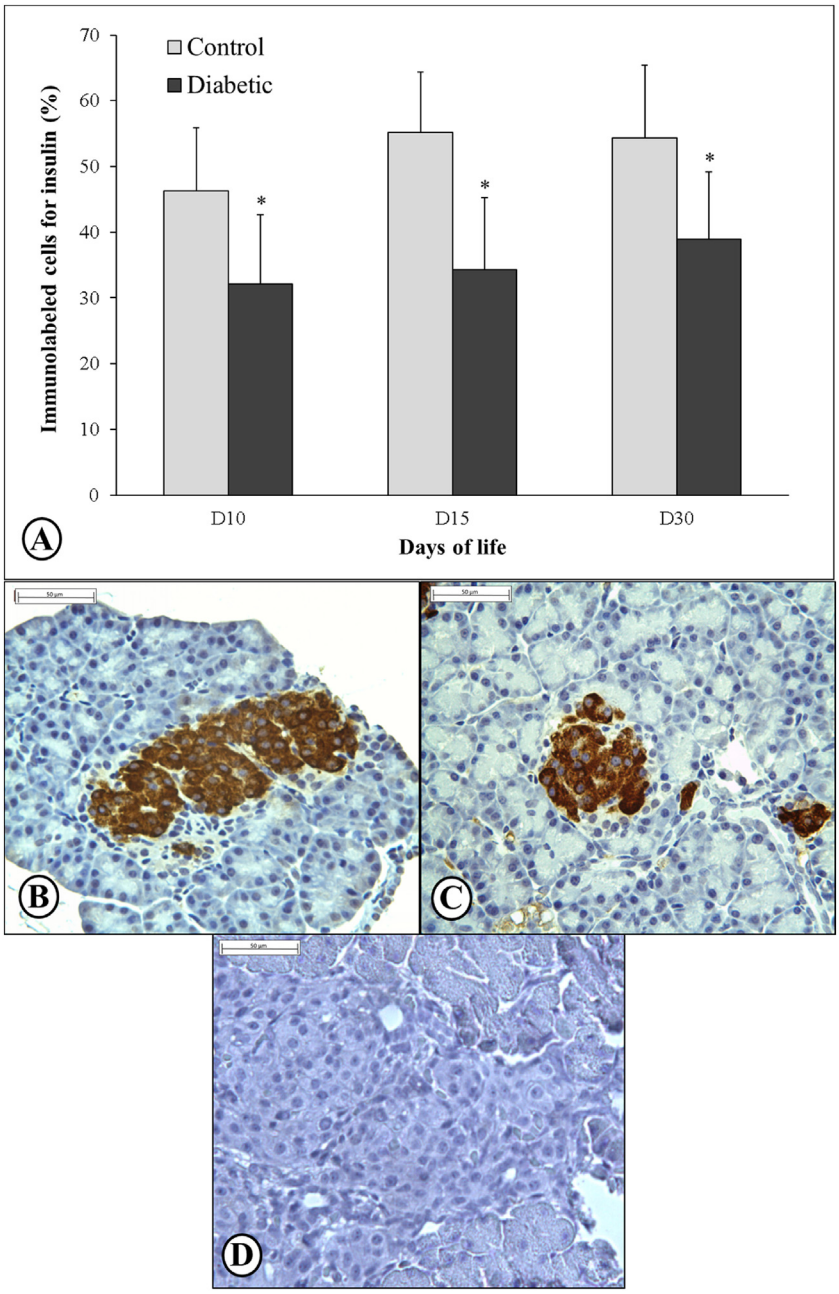

Fig. 5. Immunostaining for insulin (β-cells) in the pancreatic islets of the control and STZ animals. A- Percentage of immunolabeled cells for insulin in the control and STZ groups at different moments of life (days 10, 15 and 30 of life) (n = 100 islets/group). B- Immunohistochemistry micrograph of insulin, β-cells are located in the center of the pancreatic islet of the control group (D30) (40× magnification). C- The same location of β-cells is seen pancreatic islet of the STZ group (D30) (40× magnification). D- Negative control for insulin immunohistochemistry (40× magnification).
Data expressed as the mean ± standard deviation (*Poisson Distribution*).
* p < *0.05 - compared to the Control group*.

counterstained in Mayer's hematoxylin and mounted.

The images were captured using the computerized image system (Software KS-300, version 3.0, Zeiss®), integrated to digital camera image (CCD-IRIS/RGB, Sony®, China), and microscope (DMR, Leica®, Brazil). The cells of the pancreatic islets were identified and classified by the presence of cytoplasmic labeling for the antibodies insulin, glucagon and somatostatin. Cell counts were performed using ImageJ® software (NIH, USA). The percentage of cells present in each pancreatic islet was calculated by the ratio between the number of immunolabeled cells and the number of total cells and the value obtained was multiplied by 100. Because GSH-Px and SOD-1 are present in all endocrine pancreatic cells, the analysis of these antioxidant enzymes was performed by the intensity of immunostaining by ImageJ®.

2.5. Statistical analysis

All analyses were carried out with the assistance of the Biostatistics specialist at the Office of Research Support (EAP) of the Faculty of Medicine of Botucatu, Unesp. A completely randomized design was used to calculate the sample size (n), with an “n” of 10 animals/group established for each period of life. For immunohistochemical analysis, the calculation was estimated in six animals/group for each period, with a minimum of 10 islets/animal/pancreas. For comparison between serum insulin and glucagon concentrations, Gamma Distribution Test was used. The area and percentage of cells immunolabeled for insulin, glucagon, and somatostatin was analyzed by Poisson. The relative weight of the pancreas was analyzed by Tukey's Multiple Comparison Test. Pearson's correlation was used to analyze the correlations between the percentage of cells immunolabeled for insulin, somatostatin, and glucagon. The labeling intensity for Superoxide Dismutase 1 (SOD-1) and Glutathione Peroxidase (GSH-Px) was analyzed by the Gamma Distribution test. For all comparisons, it was considered the minimum limit of the statistical significance of $p < 0.05$.

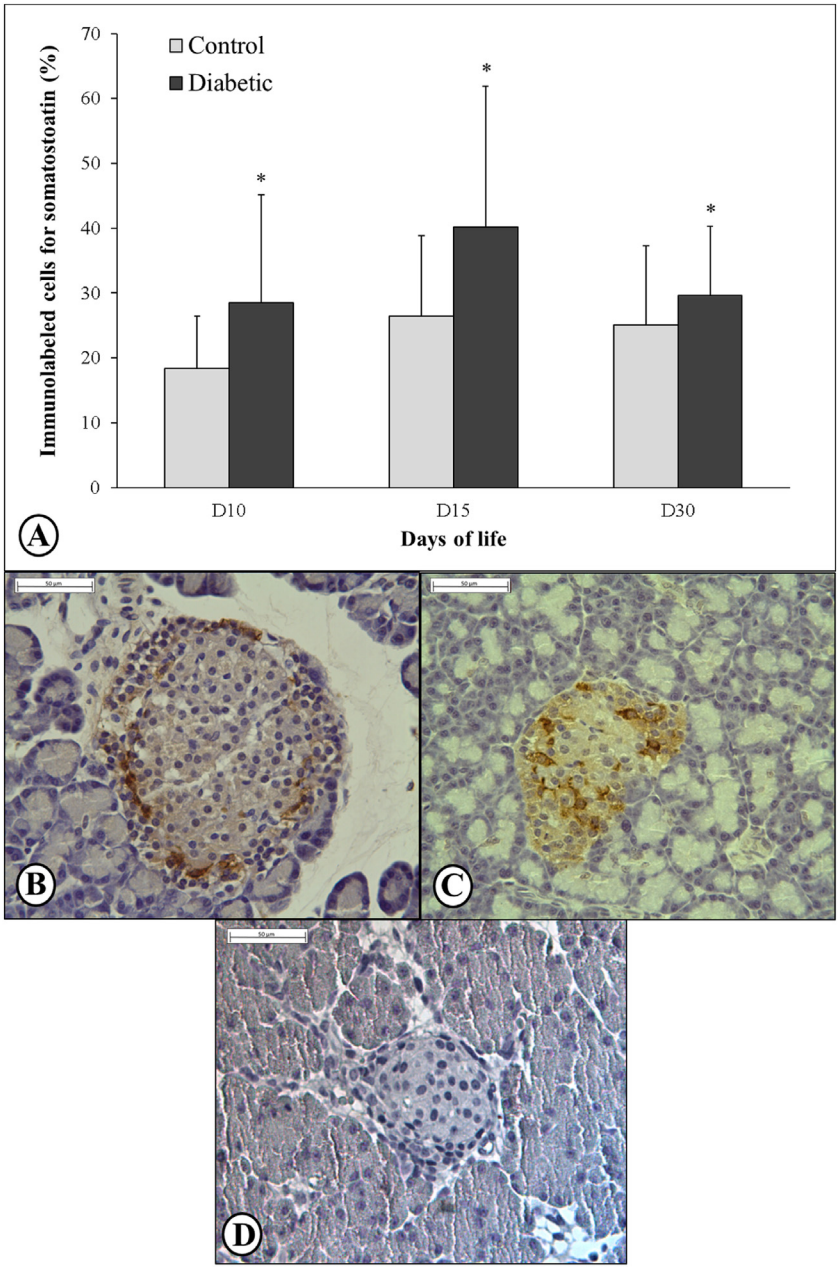

Fig. 6. Immunostaining for somatostatin (δ-cells) in the pancreatic islets of the control and STZ animals. A- Percentage of immunolabeled cells for somatostatin comparing the control and STZ groups at different moments of life (days 10, 15 and 30 of life) (n = 100 islets/group). B- Representative micrograph of immunostaining for somatostatin, showing positive cells in the periphery of the pancreatic islet in the control group (D30) (40× magnification). **C-** In contrast, immunostained cells for somatostatin are located in the center of the pancreatic islet in the STZ group (D30) (40× magnification). D- Negative control for somatostatin immunohistochemistry (40× magnification).
Data expressed as the mean ± standard deviation.
* $p < 0.05$ *- compared to the Control group* (*Poisson Distribution*).

3. Results

To confirm the STZ action on pancreatic β-cell in newborn rats, a comparative analysis was performed between STZ and control (non-diabetic) animals at D5. In comparison with the control group (glycemia = 92 ± 20 mg/dL), the STZ animals showed higher glycemic levels (520 ± 118 mg/dL) at D5 ($p < 0.0001$). These animals also showed higher insulin (STZ = 1.03 ± 0.60 versus control = 0.21 ± 0.06 ng/mL, $p < 0.0001$) and glucagon levels (STZ = 0.74 ± 0.34 versus control = 0.43 ± 0.08 ng/mL, p = 0,005). In relation to the morphological analysis, the STZ rats showed abnormal distribution of pancreatic endocrine cells characterized by circular shape and presenting extensions around them, covering not only the cells of the endocrine pancreas but also cells of the duct and acini (Fig. 2). STZ animals presented a decreased area of pancreatic islets compared to control group (STZ = 5058 ± 2680 versus control = 7115 ± 2245 pixels^2, p = 0,0023). There was a lower percentage of β-cells (STZ = 27.34 ± 7.95 versus Control = 50.50 ± 8.75, $p < 0.0001$) and a higher percentage of cells immunolabeled for glucagon (STZ = 49.07 ± 11.96 versus Control = 27.29 ± 8.45, $p < 0.0001$) and somatostatin (STZ = 30.31 ± 10.45 versus Control = 16.51 ± 6.58, $p < 0.0001$). In relation to the antioxidant enzymes, the STZ rats showed a decrease in the labeling intensity for SOD-1 in relation to the control (STZ = 4707 ± 1941 versus Control = 229,915 ± 185,114, $p < 0.0001$) at D5 (Supplementary material).

The serum insulin concentration of the control and STZ animals in D10, D15, and D30 is shown in Fig. 3A. The STZ rats presented lower serum insulin concentration in D15 when compared to the control group (Fig. 3A). In relation to the serum glucagon concentration, there were higher levels of this hormone in D30 in relation to the other days of the control group. The STZ rats had higher glucagon levels on D10 and D15 when compared to the respective days of the control group (Fig. 3B).

Fig. 4 shows the area of the pancreatic islets on the different days of control and STZ groups. At all the evaluated moments (D10, D15 and D30) the animals of the STZ group presented smaller pancreatic islet

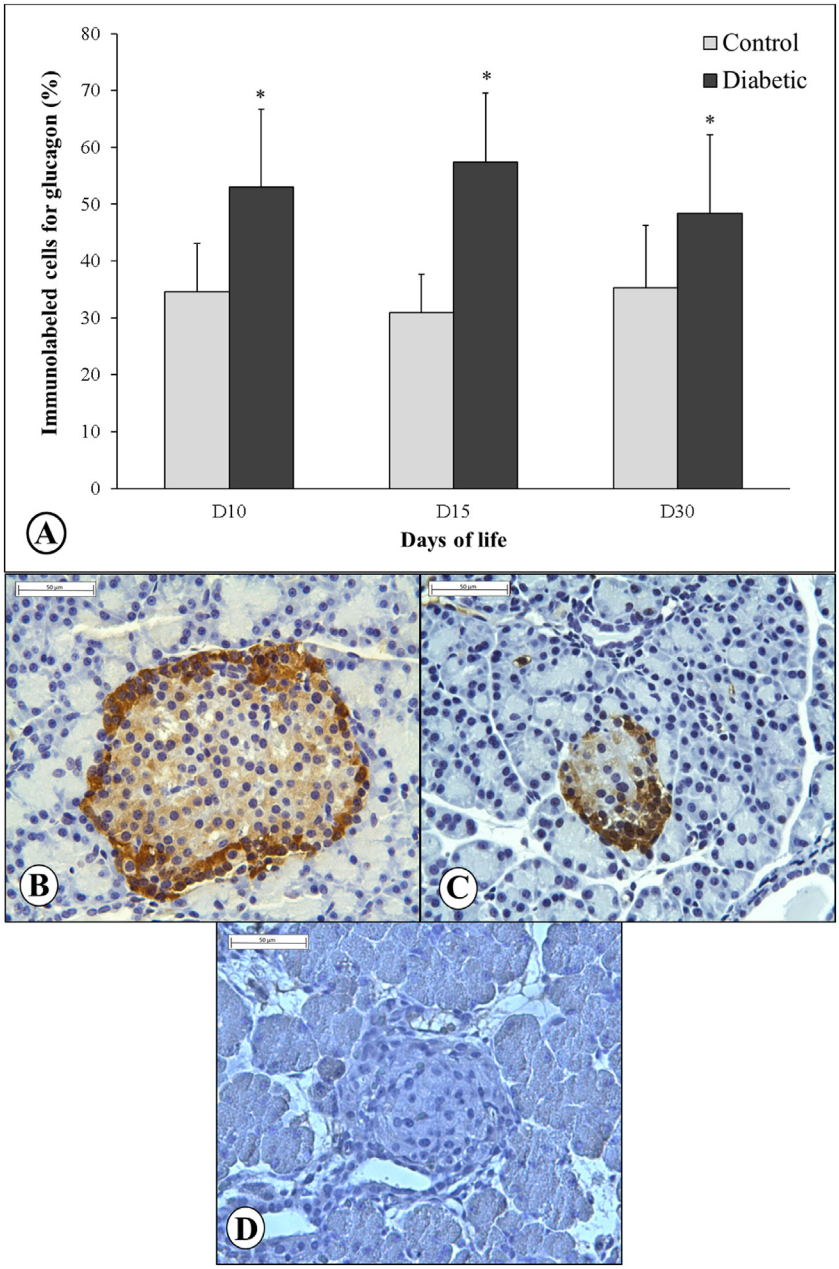

Fig. 7. Immunostaining for glucagon (α-cells) in the pancreatic islets of the control and STZ animals. A- Percentage of cells immunolabeled for glucagon from the control and STZ groups at different moments of life (days 10, 15 and 30 of life) (n = 100 islets/group). B- Cells that showed immunostaining for glucagon are in the periphery of the pancreatic islet of the control group (D30) (40× magnification). C- In contrast, in STZ animals immunostained cells for glucagon are in the periphery and some of them are near to the center of the pancreatic islet (D30) (40× magnification). D- Negative control for glucagon immunohistochemistry (40× magnification).
Data expressed as the mean ± standard deviation.
* p < *0.05 - compared to the Control group* (*Poisson distribution*).

Table 1
Correlation among the percentage of β, α, δ-pancreatic cells on different moments of life (days 10, 15 and 30 of life).

	D10		D15		D30	
β cell · α cell	r^2 = - 0.32787	(p = 0.001)	r^2 = - 0.48011	(p < 0.0001)	r^2 = - 0.50396	(p < 0.0001)
β cell · δ cell	r^2 = - 0.37485	(p = 0.0015)	r^2 = - 0.15599	(p = 0.1670)	r^2 = - 0.2163	(p = 0.0729)
α cell · δ cell	r^2 = 0.50793	(p = 0.0002)	r^2 = 0.22550	(p = 0.0443)	r^2 = 0.20436	(p = 0.0897)

Pearson's Correlation.

area compared to control group.

The STZ rats presented lower percentage of β-cells than the control group on all evaluated days (Fig. 5A). Independently of the group (control or STZ), the β-cells were located in the center of the pancreatic islet (Fig. 5B and C, respectively).

Concerning the percentage of δ-cells (Fig. 6), the STZ group showed a higher percentage of somatostatin-immunolabeled cells at all evaluated moments when compared to the control group (Fig. 6A). In the control group, somatostatin-immunolabeled cells remained at the periphery of the pancreatic islet (Fig. 6B), and higher amount of δ-cells were seen dispersed within the pancreatic islets of STZ rats (Fig. 6C).

In the pancreas of the STZ rats, there was a higher percentage of α-cells on all evaluated days compared to the control group (Fig. 7A), being located at the periphery of the islets (Fig. 7B and C).

Table 1 presents the correlations between the different cell types (β, δ, α) on D10, D15, and D30. Regarding the correlation between the percentage of β and α cells, a negative correlation was observed in all the studied days (Table 1). There was a significant negative correlation

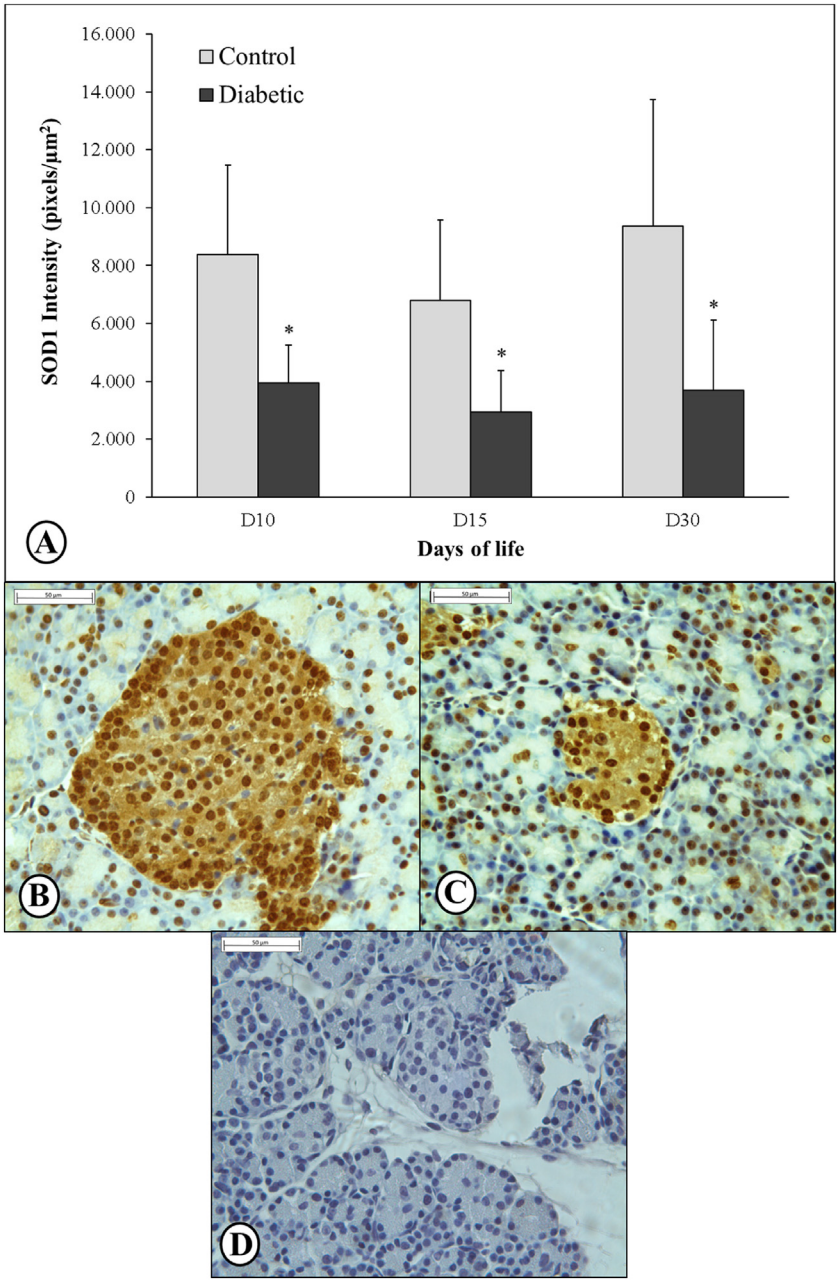

Fig. 8. Immunostaining for SOD-1 in the pancreatic islets of the control and STZ animals. A- Intensity of labeling for SOD-1-immunolabelled cells in the pancreatic islets of the control and STZ animals at different moments of life (days 10, 15 and 30 of life). B- Nuclear and cytoplasmic immunostaining for SOD-1 in the pancreatic islet of the control group (D30) (40× magnification). C- Nuclear and cytoplasmic immunostaining for SOD-1 in the pancreatic islet of the STZ group (D30) (40× magnification). D- Negative control for SOD-1 immunohistochemistry (40× magnification).
Data expressed as the mean ± standard deviation.
* p < *0.05 - compared to the Control group* (*Gamma Distribution*).

between the percentage of cells β and δ on D10. A positive correlation was found between α and δ-cells on D10 and D15.

The STZ rats presented lower SOD-1 labeling intensity in D10, D15, and D30 compared with those of the control group (Fig. 8). As for GSH-Px, the STZ group had lower labeling intensity in D10 and D30 (Fig. 9) when compared to the control group.

The STZ rats presented two altered glycemic points (30 and 60 min) in relation to the control group during OGTT (Fig. 10A). There was a significant difference in AUC between both groups (Fig. 10B). In addition to the glycemia changes observed after glucose overload, STZ animals at D30 presented higher concentrations of fructosamine (STZ = 102.35 ± 4.71 versus control = 73.31 ± 3.19 µmol/L), confirming hyperglycemia in these animals during the last three weeks.

4. Discussion

The present study showed that endocrine cells from pancreatic islets of STZ-injected rats undergo temporal structural changes, especially in the δ-cell location. There are also functional alterations (reduction of the antioxidant enzymes) that lead to the development of diabetes during postnatal critical development window.

The structural alterations after STZ administration have seen observed at D5 of life presenting a reduced islet area and loss of the cytoarchitecture. In addition, the animals presented severe hyperglycemia (glycemia ≥400 mg/dL) and hyperinsulinemia. The STZ-induced β-cell necrosis is related to pre-proinsulin and proinsulin release, increasing the insulin levels in these animals, which were detected by assay performed. The commercial kit used in this study was not specific for only insulin content, but pre-proinsulin and proinsulin release after the β-cell death. Thus, this fact could explain the hyperinsulinemic status on D5 of STZ-injected rats.

After the initial injury caused by STZ action, at days D10, D15 and D30 of life, the islets area remained decreased and the shape was restored. However, the δ-cell location remained ectopic, spread among β-cells, in the center of the islets, damaging the mantle-core structure present in rodents. Several studies with STZ analyzed the changes in α

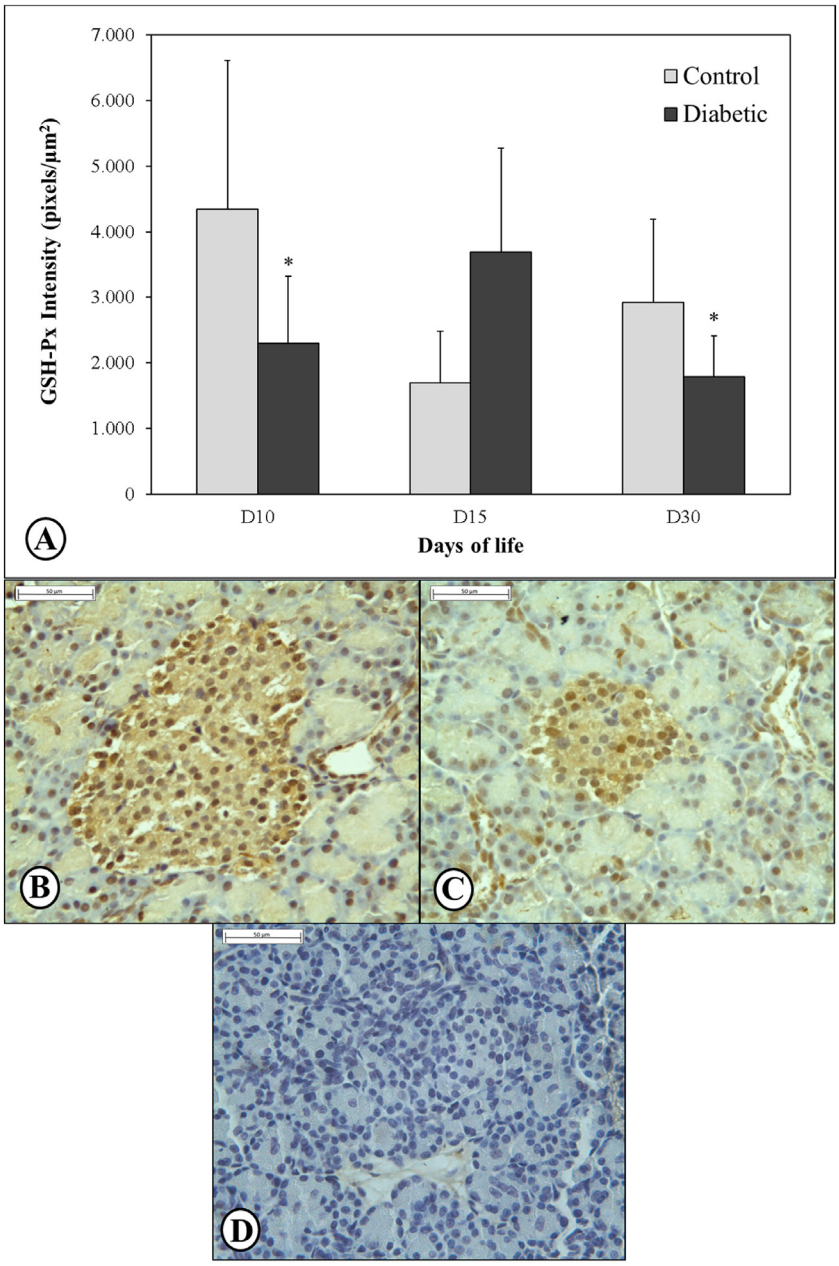

Fig. 9. Immunostaining for GSH-Px in the pancreatic islets of the control and STZ animals. A- Intensity of labeling for GSH-Px-immunolabeled cells in the pancreatic islets of the control and STZ animals at different moments of life (days 10, 15 and 30 of life). B- Nuclear and cytoplasmic immunostaining for GSH-Px in the pancreatic islet of the control group (D30) (40× magnification). C- Nuclear and cytoplasmic immunostaining for GSH-Px in the pancreatic islet of the STZ group (D30) (40× magnification). D- Negative control for GSH-Px immunohistochemistry (40× magnification).
Data expressed as the mean ± standard deviation.
* $p < 0.05$ - *compared to the Control group* (*Gamma Distribution*).

and β-cells [26,30,31]. Thyssen et al. [26] using STZ-injected rat at day 4 of life verified colocalization of glucagon with either Pdx-1 or Glut-2 in STZ-treated animals, indicating that α-cells are involved in the regeneration of β-cells. The ectopic activity of Pdx-1, combined with other factors, may be part of the mechanism of conversion of α and acinar cells as insulin producer. Pdx-1 binds to glucagon and insulin promoters, inhibiting glucagon expression and inducing insulin transcription [32–35]. Liang et al. [30] also observed the ability of α-cells dedifferentiated into endocrine precursor cells after STZ administration in neonatal period. Although other studies have evaluated the α and δ-cell regeneration after STZ administration in adult mice [36,37], the data not suggest a replacement of β-cells derived by reprogrammed α-cell in adult life [26,30]. However, another study using diphtheria toxin for β-cell extreme loss presented colocalization of insulin and glucagon in islets in adulthood [38], which shows that β-cell restoration from α-cell reprogramming is related to neonatal period or after β-cell extreme loss (99%).

Our data demonstrated a negative correlation between the percentage of labeled cells for insulin and somatostatin at the day 10 of life, inverse relationship between β- and α-cells on all days studied and positive correlation between α and δ-cells on days 10 and 15. These findings suggest that α and δ-cells may be reprogrammed into another cell type.

Despite on structural changes observed until D15, the lower serum insulin and higher glucagon levels show that at this stage the pancreas was unable to restore basal insulin secretion. An increase in the labeling pattern of the enzyme glutathione peroxidase was possibly attempting to compensate alterations in redox status during the remodeling of the pancreatic islets. However, this was not sufficient since the immunolabeling with insulin was reduced and there was an increase in the glucagon and somatostatin labeling in all periods analyzed. In addition, the experimental model used in this study showed that STZ-induced diabetic rats had a decrease in the intensity of labeling for SOD-1 at all evaluated times and a decrease in GSH-Px on days 10 and 30 of life. Oxidative stress associated with decreased antioxidant enzymes has been observed in studies with clinical and experimental diabetes [39,40]. The β-cells from adult male rats were isolated and placed at different concentrations of glucose to analyze the antioxidant enzymes

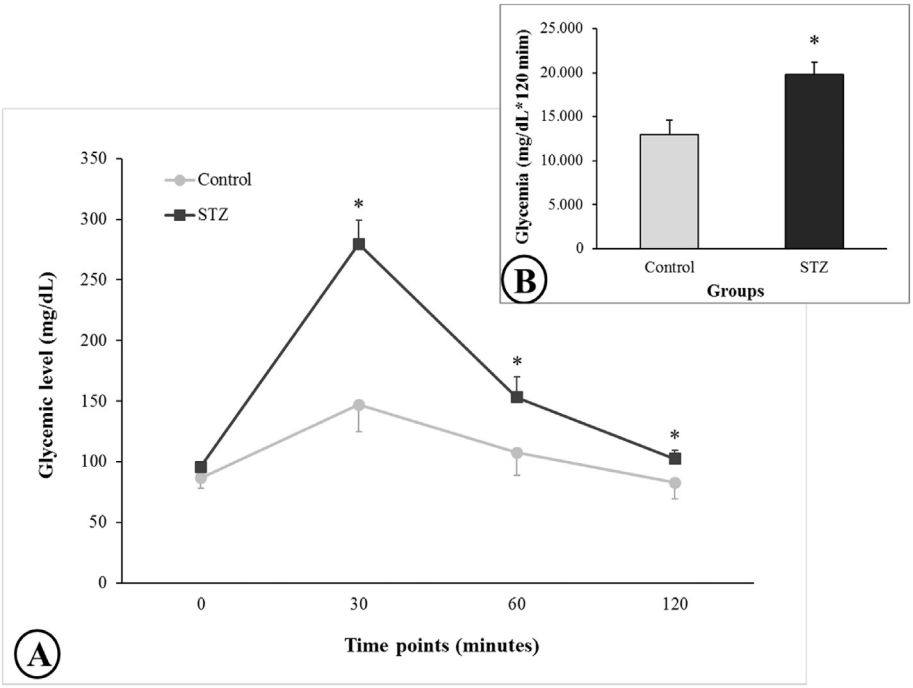

Fig. 10. A - Oral Glucose Tolerance Test (OGTT). B - Area under the curve of control and STZ rats on day D28 of life.
Data expressed as the mean ± standard deviation (n = 10 animals/group).
* p < *0.05 - compared to the control group (t-Test with repeated measures for OGTT and t-Test for area under the curve - AUC).*

and the presence of ROS. β-cells, responsive to glucose, present a decrease in SOD levels at high glucose concentrations (300 mg/dL) [41]. However, in this study, our evaluation with lipoperoxidation biomarkers is necessary to confirm the oxidative stress in diabetic animals during the first month of life.

These endocrine pancreatic changes are occurring in the attempt to control glycemic levels after insult in the pancreas. This fact can be confirmed by the basal insulin levels, which were restored from D30 of life since in fasting glycemia of the rats (control versus STZ) showed no differences. However, after a glucose overload in OGTT, the STZ rats presented high glycemic levels and no glycemic return at the end of this test, confirming diabetic status in the first month of life after STZ injury.

5. Conclusion

In conclusion, after destruction of pancreatic β-cells on the first day of life by STZ, there was a response of the pancreas to restore the basal glucose and insulin levels in the first month of life. However, the animals presented abnormal distribution in the number of β-, δ- and α-cells, decreased islet area with ectopic δ-cells and a decline of antioxidant enzymes. This fact contributed to an increased susceptibility of cells to hyperglycemia-induced ROS in this postnatal critical development window and onset of diabetes from day 30 of life of rats.

Supplementary data to this article can be found online at https://doi.org/10.1016/j.lfs.2019.03.061.

Acknowledgments

The authors grant Mr. Danilo Chaguri, the technician responsible for the Laboratory of Experimental Research in Gynecology and Obstetrics for the handling of the animals and assistance in the surgeries; Mr. Eduardo Kloppel for oxidative stress biomarker measurements, and Prof. Dr. José Eduardo Corrente for design and statistical analysis.

Funding

This research was supported by the São Paulo Research Foundation (FAPESP - Protocol Number 2011/18519-7). This study was financed by the Coordination for the Improvement of Higher Education Personnel (CAPES) – Financial Code 001 for the fellowship to F.Q. Gallego.

Conflict of interests

The authors declare that there are no conflict of interest.

Author contributions

Franciane Quintanilha Gallego, Yuri Karen Sinzato, Carolina Abreu Miranda and Débora Cristina Damasceno designed the study. Franciane Quintanilha Gallego, Yuri Karen Sinzato, Carolina Abreu Miranda, Isabela Lovizutto Iessi and Bruna Dallaqua collected the data. Franciane Quintanilha Gallego, Yuri Karen Sinzato, Carolina Abreu Miranda, Gustavo Tadeu Volpato and Débora Cristina Damasceno performed all statistical analyses and interpreted the data. Franciane Quintanilha Gallego, Yuri Karen Sinzato, Gustavo Tadeu Volpato, Rogelio Hernandez Pando, Noeme Souza, Débora Cristina Damasceno drafted the work and performed final revision of the intellectual content. All authors were responsible for critical revisions and approved the final version of the manuscript.

References

[1] S. Kordowich, A. Mansouri, P. Collombat, Reprogramming into pancreatic endocrine cells based on developmental cues, Mol. Cell. Endocrinol. 323 (2010) 62–69, https://doi.org/10.1016/j.mce.2009.12.016.
[2] M.F. Brereton, E. Vergari, Q. Zhang, A. Clark, Alpha-, Delta- and PP-cells: are they the architectural cornerstones of islet structure and coordination?, J. Histochem. Cytochem. 63 (2015) 575–591. doi:https://doi.org/10.1369/0022155415583535.
[3] S. Bonner-Weir, B.A. Sullivan, G.C. Weir, Human islet morphology revisited: human and rodent islets are not so different after all, J. Histochem. Cytochem. 63 (2015) 604–612, https://doi.org/10.1369/0022155415570969.
[4] S. Bonner-Weir, L. Orci, New perspectives on the microvasculature of the islets of Langerhans, Diabetes 31 (1982) 883–889, https://doi.org/10.2337/diab.31.10.

883.
[5] E. Samols, S. Bonner-Weir, G.C. Weir, 2 intra-islet insulin-glucagon-somatostatin relationships, Clin. Endocrinol. Metab. 15 (1986) 33–58, https://doi.org/10.1016/S0300-595X(86)80041-X.
[6] L.R. Nyman, K.S. Wells, W.S. Head, M. McCaughey, E. Ford, M. Brissova, D.W. Piston, A.C. Powers, Real-time, multidimensional in vivo imaging used to investigate blood flow in mouse pancreatic islets, J. Clin. Invest. 118 (2008) 3790–3797, https://doi.org/10.1172/JCI36209.
[7] C.R. Pfeifer, A. Shomorony, M.A. Aronova, G. Zhang, T. Cai, H. Xu, A.L. Notkins, R.D. Leapman, Quantitative analysis of mouse pancreatic islet architecture by serial block-face SEM, J. Struct. Biol. 189 (2015) 44–52, https://doi.org/10.1016/j.jsb.2014.10.013.
[8] Y.M. Liu, P.H. Guth, K. Kaneko, E.H. Livingston, F.C. Brunicardi, Dynamic in vivo observation of rat islet microcirculation, Pancreas 8 (1993) 15–21, https://doi.org/10.1097/00006676-199301000-00005.
[9] C. Bousquet, J. Guillermet, F. Vernejoul, H. Lahlou, L. Buscail, C. Susini, Somatostatin receptors and regulation of cell proliferation, Dig. Liver Dis. 36 (2004) 2–7, https://doi.org/10.1016/j.dld.2003.11.007.
[10] F. Giacco, M. Brownlee, Oxidative stress and diabetic complications, Circ. Res. 107 (2010) 1058–1070, https://doi.org/10.1161/CIRCRESAHA.110.223545.
[11] S. Lenzen, The mechanisms of alloxan- and streptozotocin-induced diabetes, Diabetologia 51 (2008) 216–226, https://doi.org/10.1007/s00125-007-0886-7.
[12] S. Lenzen, J. Drinkgern, M. Tiedge, Low antioxidant enzyme gene expression in pancreatic tissues, Free Radic. Biol. Med. 20 (1996) 463–466, https://doi.org/10.1016/0891-5849(96)02051-5.
[13] M. Tiedge, S. Lortz, J. Drinkgern, S. Lesen, Relation between antioxidant enzyme gene expression and antioxidative defense status of insulin-producing cells, Diabetes 46 (1997) 1733–1742, https://doi.org/10.2337/diab.46.11.1733.
[14] A.P. Robertson, Chronic oxidative stress as a central mechanism for glucose toxicity in pancreatic islet beta cells in diabetes, J. Biol. Chem. 279 (2004) 42351–42354, https://doi.org/10.1074/jbc.R400019200.
[15] C.O. Eleazu, K.C. Eleazu, S. Chukwuma, U.N. Essien, Review of the mechanism of cell death resulting from streptozotocin challenge in experimental animals, its practical use and potential risk to humans, J.Diabetes Metab Disord. 12 (2013) 60. doi:https://doi.org/10.1186/2251-6581-12-60.
[16] L. Orci, B. Thorens, M. Ravazzola, H.F. Lodish, Localization of the pancreatic beta cell glucose transporter to specific plasma membrane domains, Science 245 (1986) 295–297, https://doi.org/10.1126/science.2665080.
[17] J. Wu, L.J. Yan, Streptozotocin-induced a type I diabetes in rodents as a model for studying mitochondrial mechanisms of diabetic b cell glucotoxicity, Diabetes Metab. Syndr. Obes. 8 (2015) 181–188, https://doi.org/10.2147/DMSO.S82272.
[18] D.C. Damasceno, A.O. Netto, I.L. Iessi, F.Q. Gallego, S.B. Corvino, B. Dallaqua, Y.K. Sinzato, A. Bueno, I.M. Calderon, M.V. Rudge, Streptozotocin-induced diabetes models: pathophysiological mechanisms and fetal outcomes, Biomed. Res. Int. 2014 (2014) 819065, https://doi.org/10.1155/2014/819065.
[19] L. Scaglia, C. Cahil, D. Finegood, S. Bonner-Weir, Apoptosis participates in the remodelling of the endocrine pancreas, Endocrinology 138 (1997) 1736–1741, https://doi.org/10.1210/endo.138.4.5069.
[20] C. Aguayo-Mazzucato, C. Sanchez-Soto, V. Godinez-Puig, G. Gutiérrez-Ospina, M. Hiriart, Restructuring of pancreatic islets and insulin secretion in a postnatal critical window, PLoS One 1 (2006) e35, https://doi.org/10.1371/journal.pone.0000035.
[21] B. Portha, C. Levacher, L. Picon, G. Rosselin, Diabetogenic effect of streptozotocin in the rat during the perinatal period, Diabetes 23 (1974) 889–895, https://doi.org/10.2337/diab.23.11.889.
[22] S. Bonner-Weir, D.F. Trent, R.N. Honey, G.C. Weir, Responses of neonatal rat islets to streptozotocin. Limited B-cell regeneration and hyperglycemia, Diabetes 30 (1981) 64–69, https://doi.org/10.2337/diab.30.1.64.
[23] R.N. Wang, L. Bouwens, G. Kloppel, Beta-cell proliferation in normal and streptozotocin-treated newborn rats: site, dynamics and capacity, Diabetologia 37 (1994) 1088–1096.
[24] H. Merzouk, S. Madani, D.C. Sari, J. Prost, M. Bouchenak, J. Belleville, Time course of changes in serum glucose, insulin, lipids and tissue lipase activities in macrosomic offspring of rats with streptozotocin-induced diabetes, Clin. Sci. (Lond.) 98 (2000) 21–30, https://doi.org/10.1042/cs0980021.
[25] S. Bonner-Weir, G.C. Weir, New sources of pancreatic beta-cells, Nat. Biotechnol. 23 (2005) 857–861, https://doi.org/10.1038/nbt1115.
[26] S. Thyssen, E. Arany, D.J. Hill, Ontogeny of regeneration of β-cells in the neonatal rat after treatment with streptozotocin, Endocrinology 147 (2006) 2346–2356, https://doi.org/10.1210/en.2005-0396.
[27] F.Q. Gallego, Y.K. Sinzato, C.A. Miranda, I.L. Iessi, B. Dallaqua, G.T. Volpato, W.R. Scarano, S. SanMartín, D.C. Damasceno, Pancreatic islet response to diabetes during pregnancy in rats, Life Sci. 214 (2018) 1–10, https://doi.org/10.1016/j.lfs.2018.10.046.
[28] T.M. Santos, Y.K. Sinzato, F.Q. Gallego, I.L. Iessi, G.T. Volpato, B. Dallaqua, D.C. Damasceno, Extracellular HSP70 levels in diabetic environment in rats, Cell Stress Chaperones 20 (2015) 595–603. doi:https://doi.org/10.1007/s12192-015-0581-4.
[29] Y.K. Sinzato, G.T. Volpato, I.L. Iessi, A. Bueno, I.M. Calderon, M.V. Rudge, D.C. Damasceno, Neonatally induced mild diabetes in rats and its effect on maternal, placental, and fetal parameters, Exp. Diabetes Res. 2012 (2012) 108163, https://doi.org/10.1155/2012/108163.
[30] X.D. Liang, Y.Y. Guo, M. Sun, Y. Ding, N. Wang, L. Yuan, W. De, Streptozotocin-induced expression of Ngn3 and Pax4 in neonatal rat pancreatic α-cells, World J. Gastroenterol. 17 (2011) 2812–2820, https://doi.org/10.3748/wjg.v17.i23.2812.
[31] B.M. Kim, Y.M. Han, Y.J. Shin, B.H. Min, I.S. Park, Clusterin expression during regeneration of pancreatic islet cells in streptozotocin-induced diabetic rats, Diabetologia. 44 (2001) 2192–2202, https://doi.org/10.1007/s001250100029.
[32] W.C. Li, M.E. Horb, D. Tosh, J.M. Slack, In vitro transdifferentiation of hepatoma cells into functional pancreatic cells, Mech. Dev. 122 (2005) 835–847, https://doi.org/10.1016/j.mod.2005.01.001.
[33] A. Fodor, C. Harel, L. Fodor, M. Armoni, P. Salmon, D. Trono, E. Karnieli, Adult rat liver cells transdifferentiated with lentiviral IPF1 vectors reverse diabetes in mice: an ex vivo gene therapy approach, Diabetologia. 50 (2007) 121–130, https://doi.org/10.1007/s00125-006-0509-8.
[34] S.K. Chakrabarti, J.C. James, R.G. Mirmira, Quantitative assessment of gene targeting in vitro and in vivo by the pancreatic transcription factor, Pdx1. Importance of chromatin structure in directing promoter binding, J. Biol. Chem. 277 (2002) 13286–13293, https://doi.org/10.1074/jbc.M111857200.
[35] B. Ritz-Laser, B.R. Gauthier, A. Estreicher, A. Mamin, T. Brun, F. Ris, P. Salmon, P.A. Halban, D. Trono, J. Philippe, Ectopic expression of the beta-cell specific transcription factor Pdx1 inhibits glucagon gene transcription, Diabetologia.; 46 (2003) 810–821. doi:https://doi.org/10.1007/s00125-003-1115-7.
[36] A. Plesner, J.T. ten Holder, C.B. Verchere, Islet remodeling in female mice with spontaneous autoimmune and streptozotocin-induced diabetes, PLoS One 9 (2014) e102843, , https://doi.org/10.1371/journal.pone.0102843.
[37] Y. Zhang, Y. Zhang, R.N. Bone, W. Cui, J.B. Peng, G.P. Siegal, H.Wang, H. Wu, Regeneration of pancreatic non-β endocrine cells in adult mice following a single diabetes-inducing dose of streptozotocin. PLoS One 7 (2012) e36675. doi:-doi:https://doi.org/10.1371/journal.pone.0036675.
[38] F. Thorel, V. Népote, I. Avril, K. Kohno, R. Desgraz, S. Chera, P.L. Herrera, Conversion of adult pancreatic alpha-cells to beta-cells after extreme beta-cell loss, Nature. 464 (2010) 1149–1154, https://doi.org/10.1038/nature08894.
[39] B.A. O'Brien, B.V. Harmon, D.P. Cameron, D.J. Allan, Beta-cell apoptosis is responsible for the development of IDDM in the multiple low-dose streptozotocin model, J. Pathol. 178 (1996) 176–181, https://doi.org/10.1002/(SICI)1096-9896(199602)178:2<176::AID-PATH433>3.0.CO;2-8.
[40] P.A. Low, K.K. Nickander, H.J. Tritschler, The roles of oxidative stress and antioxidant treatment in experimental diabetic neuropathy, Diabetes 46 (1997) S38–S42, https://doi.org/10.2337/diab.46.2.S38.
[41] G.A. Martens, Y. Cai, S. Hinke, G. Stangé, M. Van De Casteele, D. Pipeleers, Glucose suppresses superoxide generation in metabolically responsive pancreatic β cells, J. Biol. Chem. 280 (2005) 20389–20396, https://doi.org/10.1074/jbc.M411869200.